T. V. Nguyen
Student Mem. ASME.

C. E. Brennen
Mem. ASME.

R. H. Sabersky
Mem. ASME

Division of Engineering and Applied Science 104-44, California Institute of Technology, Pasadena, Calif. 91125

Funnel Flow in Hoppers

Detailed observations of funnel flows of dry granular materials in wedge-shaped hoppers of different geometries are presented. The variations of the flow regime with changes in the height of material in the hopper/vertical bin configuration, the width of the vertical bin, the hopper angle and the hopper opening width were investigated and a number of specific flow regimes identified (mass flow and several forms of funnel flow). In the first part of the paper particular attention is paid to the conditions for transition from one flow regime to another; in particular it is shown that the existence of a funnel depends not only on the hopper angle but is also strongly dependent on the geometry of the hopper/bin system. In the second part of the paper the variations in the shape of the funnel near the exit opening are explored in detail.

1 Introduction

This paper is concerned with the flow of dry, noncohesive, granular materials in hoppers. It is well known that for plane (wedge-shaped) or conical hoppers of fairly small included angle all of the granular material flows in a fairly uniform and regular way. Such devices have been referred to as "mass flow hoppers" and have been the subject of considerable study and analyses (for example, references [1–6]). The convergence of experimental observations and theoretical predictions suggests that there exists some understanding of the mechanics of granular media flow in these circumstances. However, as the included angle is increased and a vertical bin is added to the top of the inclined sides of the hopper changes occur in the flow pattern which are much less well understood. Most of the motion occurs in a central core, funnel or "rat-hole" and stagnant regions of material tend to occur near the walls of the bin or hopper. This paper presents experimental observations of funnel flows in plane hoppers with vertical bins since it is not only of fundamental interest but is also important to the hopper designer. In this regard comparison is made with some of the existing design criteria such as that proposed by Jenike [1].

The various types of flow pattern which were observed in the present experiments are indicated in Fig. 1 (also shown are the definitions of θ_w, D, W, and H, the hopper angle and opening width, the bin width, and the total height to the upper free surface, respectively). Fig. 2(a) is an example of type A or mass flow. The flows with stagnant regions are subdivided into two basic types, B and C. Type B has

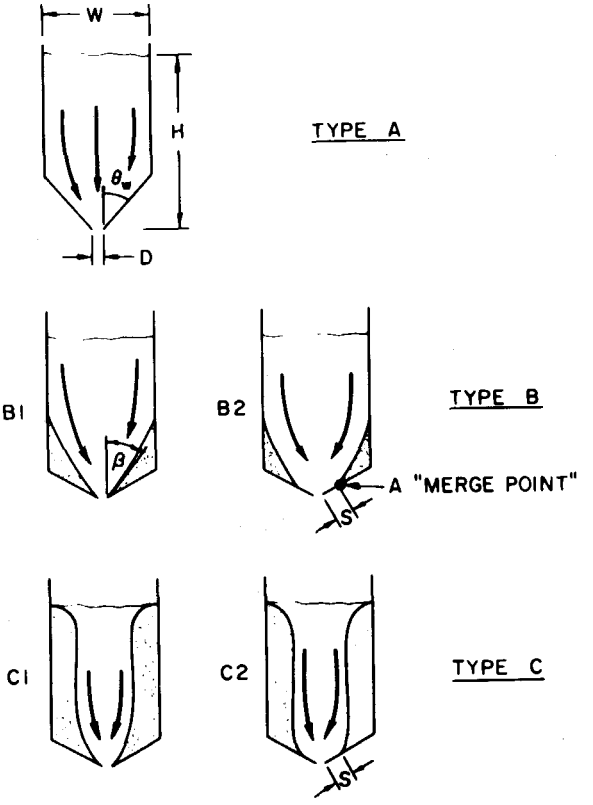

Fig. 1 Schematic indicating the different flow regimes observed. Type *A* is the mass flow regime. Types *B* and *C* are funnel flows, *B* having stagnant material in the corner and *C* having stagnant material on the sides of the bin. The geometric notation is also shown; the dimension, *b*, is the breadth of the flow or distance between the front and back vertical walls.

Contributed by the Applied Mechanics Division for publication in the JOURNAL OF APPLIED MECHANICS.

Discussion on this paper should be addressed to the Editorial Department, ASME, United Engineering Center, 345 East 47th Street, New York, N. Y. 10017, and will be accepted until March 1, 1981. Readers who need more time to prepare a Discussion should request an extension from the Editorial Department. Manuscript received by ASME Applied Mechanics Division, November, 1979; final revision, April, 1980.

Table 1 Material properties (angles in degrees)

Material	Bulk Specific Gravity	Mean Diameter mm	Internal Friction Angle	Wall Friction Angle Lucite Wall	Wall Friction Angle Aluminum Wall	θ_{w_1} (*)	θ_{w_2} (*)
Sand	1.5	0.5 -1	31	15	18	40	70
Polystyrene	0.56	0.25-0.39	39	12	17	35	60
Glass Beads	1.46	0.325	25	15.3	17.7	30	50
Rice	0.8	-	30	-	-	55	70

(*) Values of θ_{w_1} and θ_{w_2} are for a smooth walled hopper with a thickness equal to 15.2 cm.

sliding along the upper part of the bin wall and stagnant regions near the bin/hopper wall corner (for example Fig. 2(*b*)). Type *C* has no sliding along the bin walls and larger stagnant regions on either side of the funnel (for example Fig. 2(*c*) and (*d*)). Two subtypes were also noted. In some instances slip occurred along the walls of the hopper (types *B*2 and *C*2) whereas in other cases the stagnant regions extended to the opening (types *B*1 and *C*1). Figs. 2(*b*) and 2(*d*) are representative of types *B*2 and *C*2 whereas Fig. 2(*c*) is of type *C*1.

Though there have been many observations of funnel flow patterns in both plane hoppers [1, 7–9, 11, 12] and conical hoppers [16–19] the variations with hopper geometry have not been exhaustively explored. The main objective of the present investigation was to study the flow fields occurring in plane hoppers over a wide range of geometries of a hopper/vertical bin system and for a wide range of cohesionless granular materials. Some effects of rough and smooth walls are also studied.

2 Experimental Apparatus

A plane hopper surmounted by a vertical bin was made of lucite. The dimensions *H*, *W*, *D*, θ_w (see Fig. 1) and the breadth or separation of the front and back vertical walls (denoted by *b*) were all adjustable. The hopper angle, θ_w, could be varied continuously; exit openings, *D*, ranged from 0.5 cm to 3.8 cm and bin widths, *W*, from 17.8 cm to 33 cm. Most observations were made with a breadth, *b*, of 15.2 cm but tests with sand were also performed with breadths of 7.6 cm and 22.9 cm. In some tests the height, *H*, was maintained constant during flow by means of a second supply bin; in other tests *H* decreased naturally with discharge. Finally, a series of experiments were conducted in hoppers with rough inclined walls and smooth vertical walls in order to observe the effects of inclined wall roughness.

The granular materials used were sand, glass beads, polystyrene pellets and rice; the grain shapes range from spherical (glass beads) to elongated (rice). The grain size distributions were fairly uniform and all the materials are practically cohesionless. Their physical properties, measured according to the procedures described by Pearce [20], are shown in Table 1.

3 Observation of the Transition Between Flow Patterns

The transition criteria for the flow of sand in a hopper of breadth, b = 15.2 cm will be discussed first. When the hopper angle, θ_w, was less than about 60° mass flow (type *A*) was observed to occur until the free surface reaced a critical height, *H*. Below this value of *H*, stagnant side flow of type *C* occurred. In Fig. 3, the critical ratio *H*/*W* is plotted

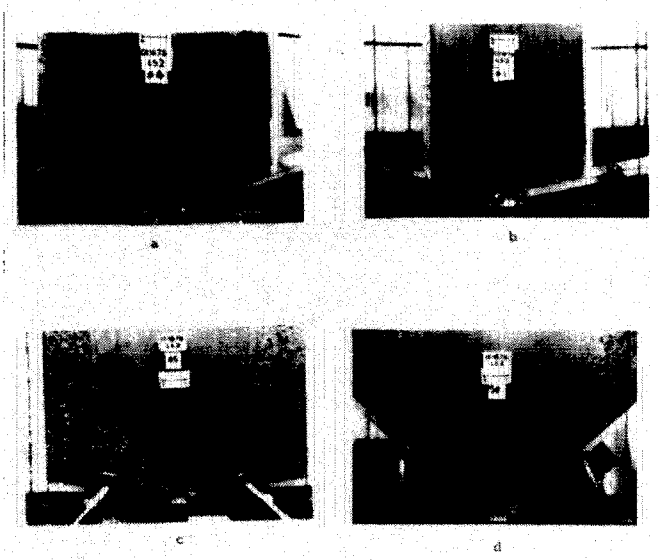

Fig. 2 Photographic examples of the flow patterns for the sand ($\varphi = 31°$). The breadth, *b*, is 15.2 cm in all cases. The following are the values of θ_w, *H*, *W*, *D* (in cm): (*a*) 70°, 36.8, 22.9, 1.91 (*b*) 80°, 58.4, 17.8, 1.37 (*c*) 70°, 35.6, 30.5, 2.54 (*d*) 50°, 35.6, 30.5, 2.54.

versus the ratio *W*/*D* for various hopper angles. For θ_w less than about 60°, the critical value of *H*/*W* is more or less constant for all angles θ_w. This implies that the transition from mass flow to type *C* is caused by the presence of the vertical bin on top of the hopper rather than by the inclination of the hopper walls.

For hopper angles greater than about 60°, flow of type *B* occurred for large *H*. However, the flow underwent a transition of type *C* when *H*/*W* reached the critical values plotted in Fig. 3. Again, the critical value is more or less independent of the hopper angle. (Note that even

Nomenclature

b = hopper breadth
D = width of exit opening
H = height of material above the exit opening
S = distance along side wall from edge of exit opening to merge point
W = hopper width
X = dimensionless horizontal position of funnel boundary
Y = dimensionless vertical position of funnel boundary
β = inclination of funnel to vertical at the discharge
θ_w = hopper angle

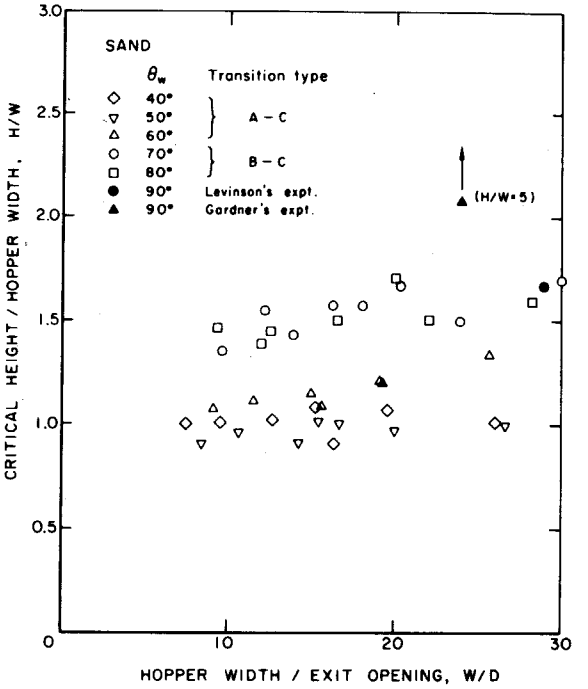

Fig. 3 Critical values of *H/W* plotted against *W/D* for various hopper angles, θ_w; the material is sand ($\varphi = 31°$, $d = 0.5 \rightarrow 1$ mm)

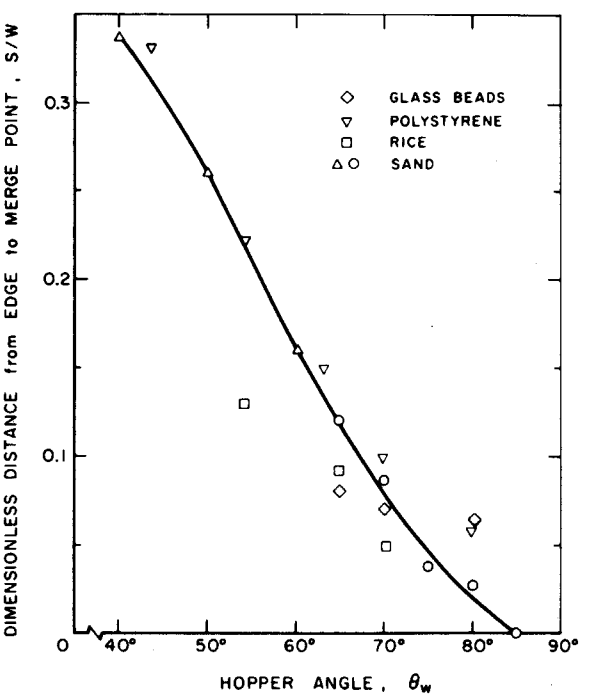

Fig. 4 Dimensionless hopper wall slip length, *S/W* plotted against the hopper angle, θ_w, for type *C* flow of the four materials used in the experiments

for hopper angles as large as 70° mass flow can occasionally occur at large H/W and small W/D).

It is important to emphasize that type C flow can be clearly distinguished from type B. The former does *not* occur simply as a result of the upper free surface engulfing the boundary between stagnant and flowing material in type B. The extent of the stagnant material distinctly increases in a B to C transition as can be seen by comparing the boundary geometries in Figs. 8 and 9.

In type B or C flow the stagnant material may either terminate at the discharge opening or it may end at a "merge point," S, which is some distance from the edge of the exit opening. In the latter case the material slides along the wall below the merge point. Consequently, mass flow is present in a localized region near the exit of the hopper. For convenience the subtypes $B2$ and $C2$ are defined as having a merge point on the hopper wall while in the subtypes $B1$ and $C1$ the merge point coincides with the edge of the discharge opening (see Fig. 1). The length of hopper wall over which slip occurs was measured for a variety of flows and will be denoted by S. Flows of type $B2$ (or $C2$) were observed to occur when the hopper angle was less than about 85°. As the angle is decreased below this the distance S increases monotonically as the flow begins a transition to mass flow. The magnitude of S also depended upon the width W. However the values of S/W for type C flows were primarily functions of θ_w as indicated in Fig. 4; the data for type B flows were limited and more scattered.

Fig. 5 is an alternative presentation of the information in Fig. 3. Here the minor variations with W/D are not explicitly shown. Rather the flow regimes are shown in a parametric map of H/W and θ_w. Fig. 5 is for sand and smooth walls; similar flow regime maps for glass beads and for sand with rough walls are presented in Figs. 6 and 7. Flow maps for other granular materials such as rice and polystyrene are included in reference [24]; they are qualitatively similar to Figs. 5 and 6.

These flow maps suggest that the phenomena are best described by defining three different ranges of hopper angle. When θ_w is between 0° and θ_{w_1} mass flow (type A) occurs in the flow field irrespective of the ratio H/W. For values of θ_w between θ_{w_1} and θ_{w_2}, a dual transition behavior is observed. There is first a transition from type A flow into type C flow. This is followed by a second transition from type C flow into type A flow at a lower critical value of H/W. Finally,

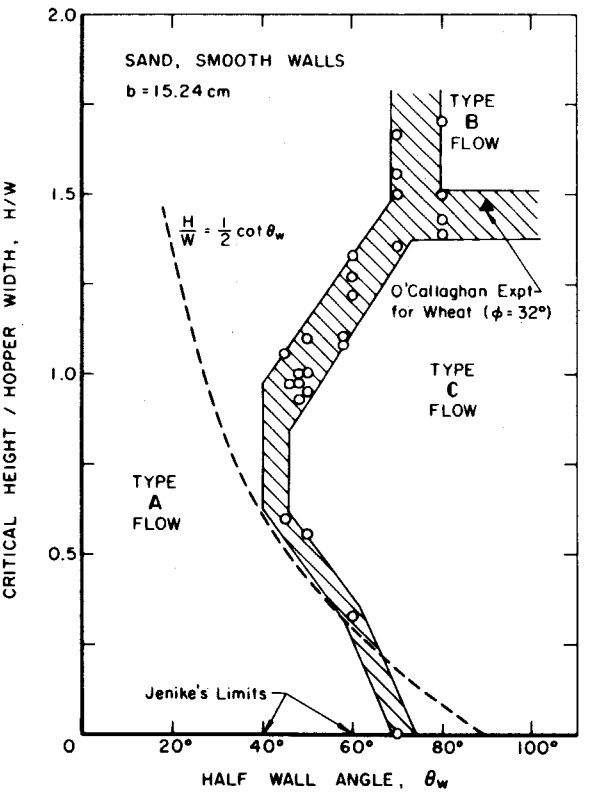

Fig. 5 Map of the flow regimes as a function of hopper geometry for the sand flowing in a smooth walled hopper. The solid lines are the approximate positions of the regime boundaries with actual transition points indicating the uncertainty in these boundaries. The dashed line locates conditions in a hopper without a bin for $W/D \gg 1$.

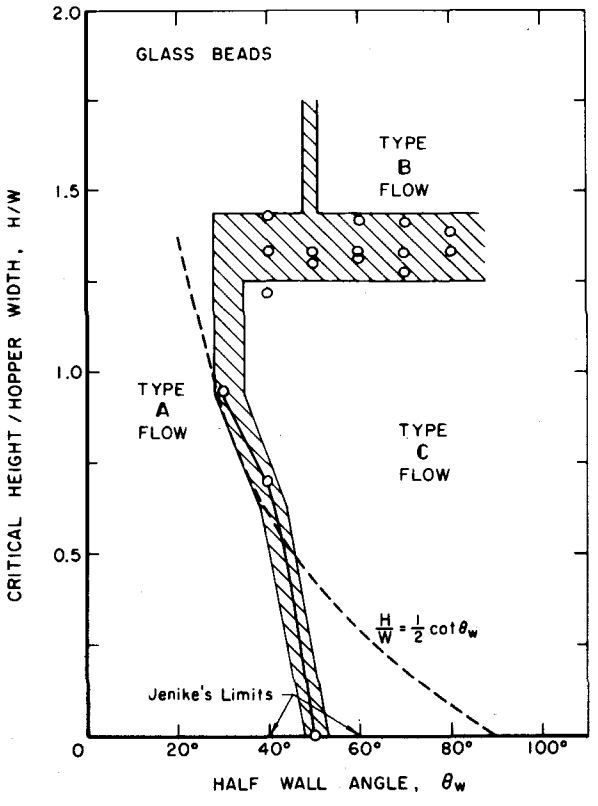

Fig. 6 Flow map as Fig. 5 but for glass beads

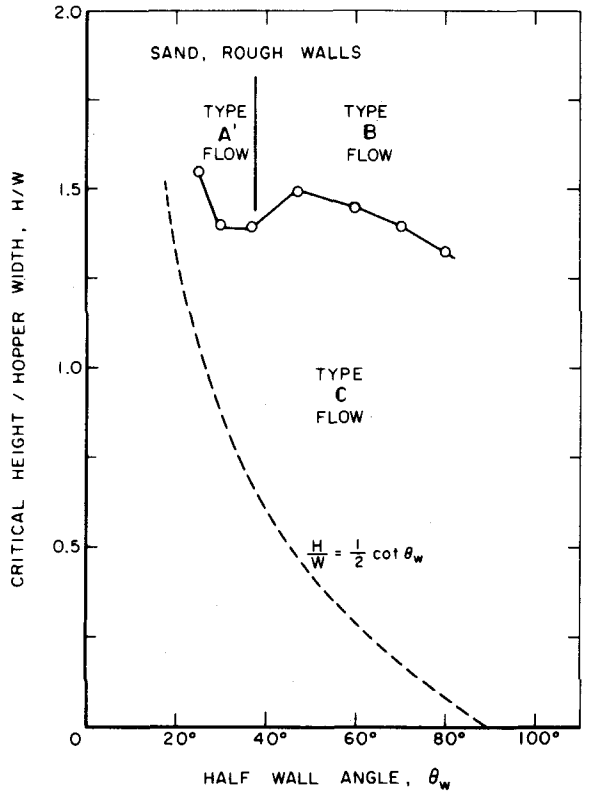

Fig. 7 Flow map as Fig. 5 but for sand in hoppers with rough inclined walls (the vertical bin walls are smooth). Type *A'* is similar to type *A* but has a thin layer of stagnant material next to the rough walls.

for values of the hopper angles θ_w greater than θ_{w2}, the transition is from type B flow into type C flow with stagnant material always present in the flow field. It should however be mentioned that some nonuniqueness can occur when the wall angles are close to the angles θ_{w1} and θ_{w2}; different flow regime histories can result for nominally identical tests. The values of θ_{w1} and θ_{w2} which appear to be functions of the frictional properties of the granular materials (and the walls) are presented in Table 1.

It follows from the foregoing that the common practice of using only values of θ_w and D as the relevant dimensions (e.g., [1]) would give a very incomplete picture of the flow field. One example is the effect of the vertical bin on the flow which can be demonstrated using the dashed lines in Figs. 5–7. These dashed lines represent the ratio H/W in a hopper without a vertical bin (for large values of W/D). Consequently such hoppers would exhibit mass flow up to the point at which the dashed line intersects that regime boundary. Note that in some cases in which a bin-less hopper exhibited mass flow (type A) the addition of a bin would change the flow regime to a funnel flow type.

As expected the material properties also play a role in determining the flow pattern. With the exception of glass beads, the higher the internal friction angle (see Table 1) of the material the lower the values of θ_{w1} and θ_{w2}. The apparent inconsistency represented by glass beads may be due to their small size (300 μm). Crewdson, Ormond, and Nedderman [21] have shown that the effects of the interstitial air can influence the discharge rate (and presumably other flow properties) when the particle size is less than about 500 μm. Other particle unique features which were noted included the tendency for the elongated rice grains to align themselves with the flow.

As previously stated the aforementioned observations were made with a breadth, b, equal to 15.2 cm. Some limited observations with breadths of 7.6 and 22.8 cm indicated the same qualitative transitional phenomena and only minor quantitative differences. Data on the variation of funnel shape with b/W are presented in Section 5 and suggests that the results have asymptoted to those of pure flow for values of b equal to 15.2 cm or greater.

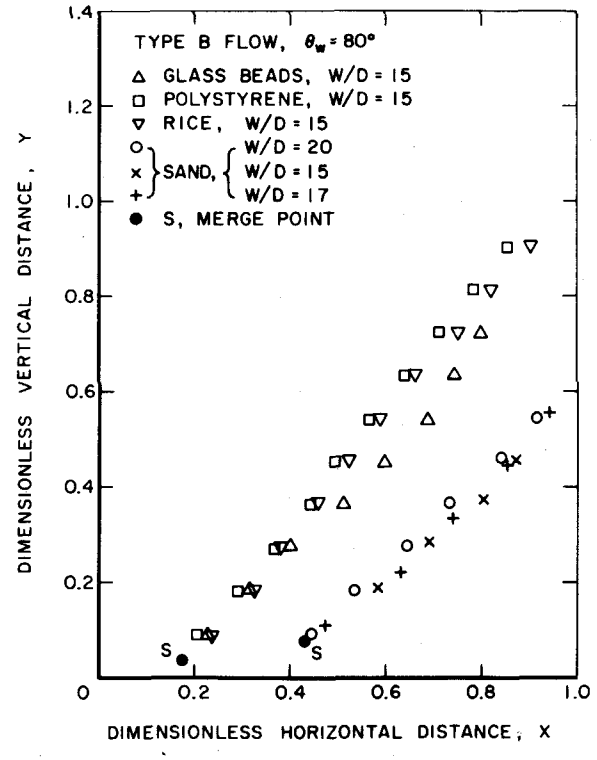

Fig. 8 Examples of funnel shapes for type *B* flows in smooth-walled hoppers (b = 15.2 cm). Shapes for given material are almost independent of θ_w, *H/W* or *W/D*.

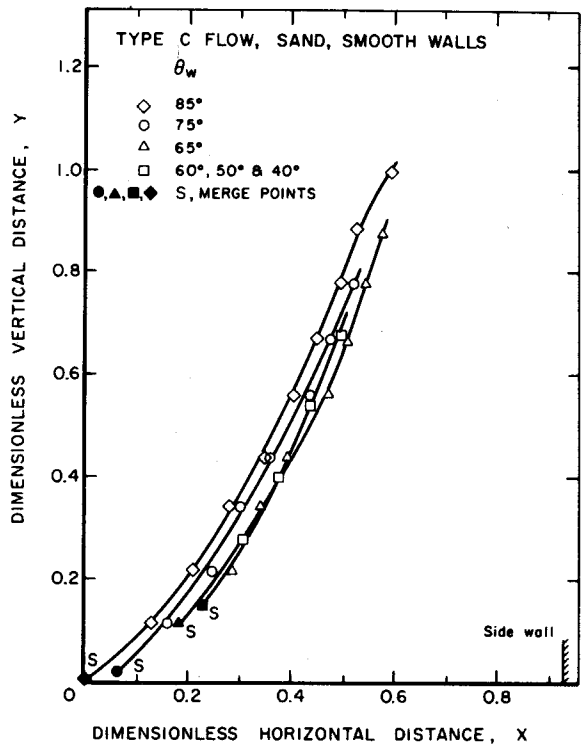

Fig. 9 Funnel shapes for type *C* flows of sand in smooth-walled hoppers of various θ_w (b = 15.2 cm)

4 Comparison With Previous Studies

Though no other complete parametric study has appeared in the literature it is valuable to compare previously observed flow patterns with those expected on the basis of the present study. O'Callaghan [7] examined the flow regimes in a flat-bottomed bin and noted the transition from type B to type C flow (which he termed "deep bin flow" and "shallow bin flow," respectively). He measured critical values for H/W of 1.47, 1.49, and 1.77 for wheat (φ = 32°), barley (φ = 38°), and fertilizer (φ = 42°), respectively. As indicated in Fig. 5 these are consistent with the present experiments. The points of operation (*not* the critical values) of the hoppers in Gardner's [8] experiments and those of Levinson, et al. [12], are shown in Fig. 3. Gardner's photographs clearly show that his flows were indeed of the type B; the values of H/W used by Levinson, et al., were marginal and this is reflected in the fact that the flows with clover seeds tended toward type B whereas, the flows with sand (which has a larger internal friction angle) were closer to type C. Though Brown and Richards [9] did not give the dimensions of their apparatus, their value of H/W appears to be about 1.5 and flows of type C were observed for a larger number of granular materials. In Toyama's [11] experiments flows of type B were encountered with large values of H/W of 10 and 6.5.

It is worth mentioning that trends similar to those previously reported for plane hoppers also appear to occur in conical hoppers. Van Zanten, et al. [16], and Giunta [18] observed flows of type C in conical systems with values of H/W of 2.57 and 1.33, respectively. On the other hand, Novosad and Surapati [19] obtained flows of type B for H/W ranging from 4 to 8. McCabe [17] observed a change in the flow field for values of H/W of about 2. Thus it would appear that conical hoppers exhibit results qualitatively similar to those reported here for wedge-shaped hoppers and that the critical value of H/W for conical hoppers is between 2 and 3 depending on the properties of the material.

Jenike [1] studied the conditions on the hopper geometry under which mass flow (type A) would occur. By balancing the stress at the exit against the strength of the material, he concluded that the *upper* limit of θ_w for which mass flow would occur was (90° − δ) or 60°, whichever is the smallest (δ is the wall friction angle). He also proposed a *lower* limit based on observations for flows in hoppers with vertical bins (and a minimum exit opening D required to avoid arching). The two limiting values of θ_w are indicated in Figs. 5 and 6 and appear to correspond roughly with the angles θ_{w_1} and θ_{w_2} of the present study. Despite a number of studies [13–15] which have questioned the validity of Jenike's critera they have been extensively used during the past 20 years for the design of bins and hoppers. We would however suggest attention also be paid to the ratio H/W since according to the present studies this appears to be a crucial parameter; we note that Johanson and Colijin [22] have introduced the concept of a minimum height, H, required to insure mass flow.

5 Variations in the Shapes of the Funnels

Having established the conditions for the $A \rightarrow C$ and $B \rightarrow C$ transitions we now proceed to examine the changes in the shape of the funnel with geometry for both type B and type C flows. In the figures which follow these shapes are plotted nondimensionally by dividing all lengths by $W/2$; the origin of the resulting X, Y coordinates in which Y is vertical is taken at the end of the hopper wall at the discharge opening. Hence type $B1$ or $C1$ profiles end at the origin. In type $B2$ or $C2$ profiles the merge points are identified by the letter S. The objective of this section will be to identify the variations in funnel shape with the parameters θ_w, H/W, W/D, b/W, and the material properties.

The dimensionless funnel shapes for type B flows were found to be almost completely independent of θ_w, H/W or H/D for a given granular material (Gardner [8] noted the lack of dependence on θ_w in his experiments). One example of this is shown in Fig. 8 where several profiles at different W and D are included for sand: other data appears in reference [24]. The profiles for different granular materials are shown in Fig. 8. The profiles for glass beads, polystyrene pellets, and rice are quite similar. Only sand appears substantially different. However this is primarily caused by a difference in the location of the merge point; relative to that point the profiles are quite similar. It is not clear why the merge point for sand should be so different from that for the other materials in type B flows; it was not the case in type C flows.

The funnels occurring in type C flow are more variable and will first be described for sand with the understanding that the results for the other materials are similar. Fig. 9 displays the type C funnel shapes in sand for various hopper angles, θ_w, at fixed values of H, W, D, and b as indicated. As one proceeds to smaller angles the type $C2$ flow slides over longer lengths of the hopper wall; this feature was previously described in Fig. 4. The funnel becomes wider but the shape of the funnel remains much the same; indeed the profiles simply appear to have been shifted outward in the X-direction. The inclination of the funnel to the vertical at the merge point, S, appears to decrease somewhat. These trends halt at θ_w = 60° and the profiles for 60°, 50°, and 40° all correspond. Hence in the type A–C transition the resulting funnel seems to be independent of the angle whereas in the type B–C transition (θ_w > 60°) the funnel shape depends on θ_w or more specifically on the position of the merge point as given by S/W.

Further type C funnel shape variations in sand are included in references [24, 25]. Briefly little or no variation in the funnel shape occurred with variations in either H/W or W/D or with changes in overall size. It was however observed that when H/W was somewhat greater than unity, the funnels were slightly larger than those for H/W < 1. This effect seems to reflect the tail end of the transition from type B flows to the type C flows.

In Fig. 10 comparison is made between the funnels for three different breadths, b, of hopper (b/W = 0.25, 0.5, and 0.75). The funnels for the two larger breadths are quite close. However, the funnel for the smallest breadth (b/W = 0.25) seems significantly narrower throughout its length. As mentioned previously, we have tentatively concluded from this that friction on the vertical front and back faces begins to alter the flow regime and funnel shape when b/W is less than some value between 0.25 and 0.4.

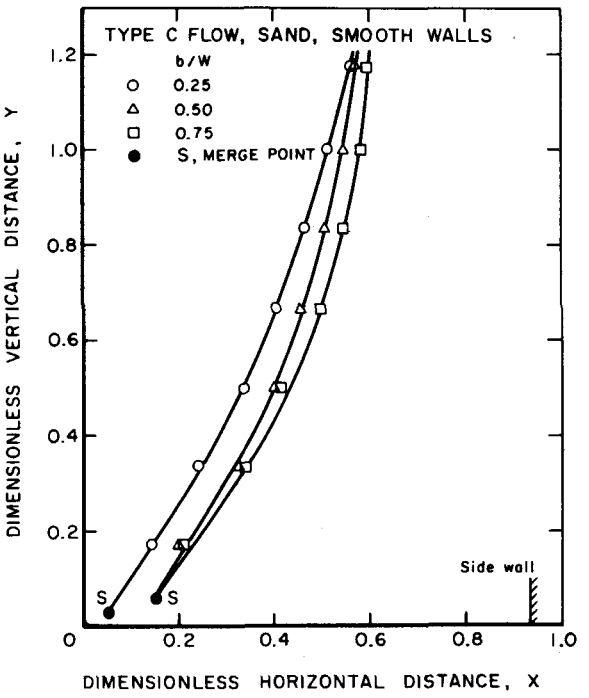

Fig. 10 Type *C* funnel shape variations with hopper breadth, *b*; for sand in smooth-walled hoppers of $\theta_w = 70°$

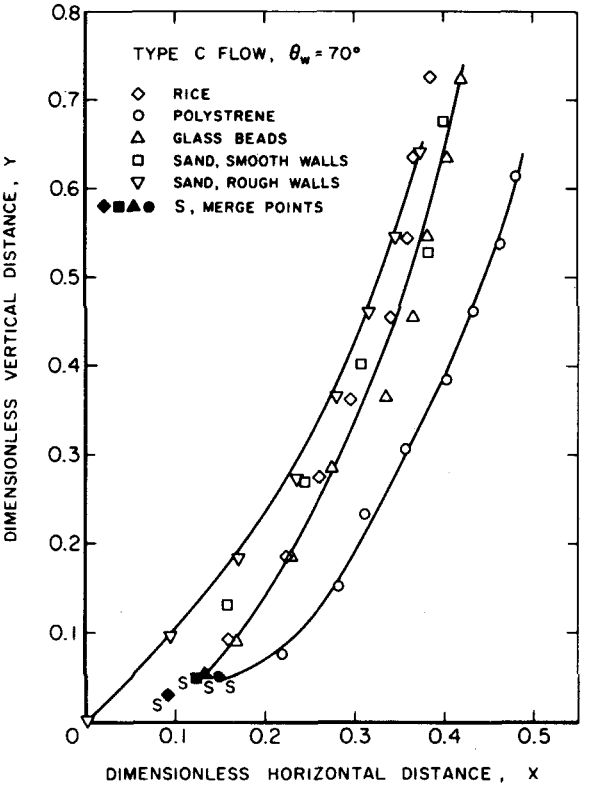

Fig. 11 Type *C* funnel shapes for different materials hopper of $\theta_w = 70°$ and $b = 15.2$ cm; funnels in sand with both smooth and rough inclined hopper walls are shown

In summary, these studies suggest that the type C funnel shapes are primarily dimensioned by the width, W, of the vertical bin. The hopper angle, θ_w, has a fairly simple effect shifting the profile outward as θ_w is decreased. Furthermore, provided the conditions are not close to the critical value of H/W for transition to another regime and provided b/W is 0.5 or larger, the funnel shape appears to be relatively independent of H/W, W/D, and b/W.

Finally a typical comparison between the type C funnel shapes in the four different granular materials is included in Fig. 10. In this respect polystyrene appears to be rather different from the other three materials.

6 The Effects of Rough Hopper Walls

It was envisaged that hopper wall roughness would affect the value of the wall friction angle and therefore the flow in the hopper, (Gardner [8], Bosley, et al. [23], and Savage and Sayed [26]). In the present study the experiments with sand were repeated in a hopper whose inclined walls were roughened by depositing sand on double-stick tape (Savage [26]). Results with vertical bin walls which were left smooth will be described here; some experiments were performed with these similarly roughened but the results dependent on the initial head of material loaded into the bin.

With rough inclined walls, a thin stagnant layer of material next to these walls was always present. Thus, at small angles θ_w, the mass flow regime will be described as type A' to denote this minor difference. Fig. 7 represents the flow map for sand in a hopper with rough inclined walls and is clearly different from that for smooth walls (Fig. 5). Even at small θ_w there appears to be a transition to type C at some critical H/W. It appears that the lower transition boundary in Fig. 7 has been rotated clockwise through about 90°. At hopper angles greater than about 40° the type B to type C transition occurs at values of H/W similar to the B–C transition for smooth walls.

The funnel boundaries in the rough-walled experiments were also insensitive to hopper geometry. It can be seen from the one example included in Fig. 11 that the primary difference between the rough and smooth wall funnels is in the location of the merge point.

It has been reported by a number of investigators (Bosley, et al. [23], and Savage and Sayed [26]), that the mass flow rate out of a hopper with rough walls can actually be *greater* than that from a similar smooth-walled hopper. Such a comparison was made in the present study, the results being presented in nondimensional form in Fig. 12 where U is the mean velocity corresponding to the discharge flow rate. It can be observed that though the smooth-walled hopper exhibits a higher flow rate at small hopper angles less than about 35°, the rough-walled hopper has the greater flow rate for $\theta_w > 35°$. Furthermore about $\theta_w = 90°$ the two converge to the same value again.

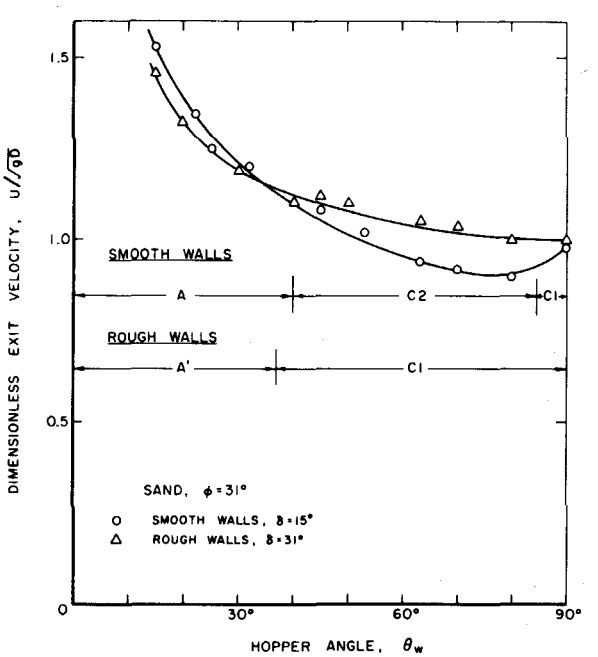

Fig. 12 The dimensionless exit velocity or discharge flow rate versus hopper angle, θ_w, for sand in hoppers with smooth and rough inclined walls

The present study revealed that such unexpected effects of wall roughness can be partially understood by reference to the different flow regimes which the two kinds of hopper exhibit over the range of hopper angles. For θ_w less than about 35°, the comparison is between types A and A'; then, as expected, the larger wall friction of the rough walls decreases the flow rate. As θ_w is increased above about 35° the rough-walled hopper produces a flow of type $C1$ in which the merge points are located at the discharge opening. On the other hand the smooth-walled hopper produces a flow of type $C2$ with merge points some considerable distance up the hopper walls. Consequently in the immediate neighborhood of discharge the flow in the rough-walled hopper experiences an "effective" hopper angle which is less than the actual hopper angle encountered in the smooth-walled hopper. Since the flow rate is primarily determined by the conditions in the flow in the immediate vicinity of discharge and since the flow rate tends to increase as the hopper angle decreases it is then possible to understand why the flow rate is greater for the rough-walled hopper.

As the hopper angle is increased further the flow rate from the rough-walled hopper changes little since its "effective" hopper angle is changing only slightly. On the other hand the actual hopper angle which is pertinent in the smooth-walled case continues to increase causing further substantial decrease in the flow rate. This continues until $\theta_w \approx 85°$ when the merge points in the smooth-walled case reach the discharge opening (see Fig. 4). At this point the flows in both types of hopper become of the type $C1$ and the flow rates converge to similar values.

Thus it can be seen that the effect of wall roughness on the flow rate is related to its effect upon the flow regime. It can also be concluded that the flow rate depends mainly upon the conditions near the exit and on the location of the merge points.

7 Concluding Remarks

In the present study, the various types of flow which exist in a hopper with a vertical bin have been identified and classified. The experimental observations show that the presence of the vertical bin will cause funnel flow to occur at lower values of the hopper wall angle θ_w. The ratio of the height of the material in the bin to its width (H/W) is important in determining the type of flow which is present and the transition from one type of flow into another.

The nondimensionalized funnel boundary is found to be independent of the hopper angle θ_w, the width of the exit opening D, and the width of the vertical bin W. It is mainly a function of the material properties. Some changes in the flow field due to the proximity of the front and back walls are observed when the hopper thickness falls below a certain limit. Finally, the presence of the wall roughness affects the flow field in the hopper by causing stagnant material to appear at lower values of θ_w. This change in the flow field is responsible for the fact that the rate of discharge from a hopper with rough walls is actually slightly *higher* than that from a hopper with smooth walls when the hopper wall angle θ_w is greater than about 35°.

Acknowledgments

The authors wish to acknowledge the contribution by Paul Mason who enthusiastically and effectively assisted in the early laboratory work. He is being sincerely missed by all of us. The authors would like to express their gratitude to the National Science Foundation for support under Grant No. ENG-7615043 and to Union Carbide Corp. for their continuing interest and financial support.

References

1 Jenike, A. W., "Storage and Flow of Solids," Bulletin No. 123, 1964, Utah Engineering Experiment Station, University of Utah, Salt Lake City, Utah.

2 Savage S. B., "Gravity Flow of Cohensionless Bulk Solids in a Converging Conical Channel," *International Journal of the Mechanical Science,* Vol. 9, 1963, p. 651.

3 Brennen, C., and Pearce, J. C., "Granular Material Flow in Two-Dimensional Hoppers," ASME JOURNAL OF APPLIED MECHANICS, Vol. 45, 1978, p. 43.

4 Nguyen, T. V., Brennen, C., and Sabersky, R. H., "Gravity Flow of Granular Materials in Conical Hoppers," ASME JOURNAL OF APPLIED MECHANICS, Vol. 46, Sept. 1979, pp. 529–535.

5 Lee, J., Cowin, S. C. and Templeton III, J. S., "An Experimental Study of the Kinematics of Flow Through Hoppers," *Transactions of the Society of Rheology,* Vol. 18, No. 2, 1974, p. 247.

6 Drescher, A., Cousens, T. W., and Bransby, P. L., "Kinematics of the Mass Flow of Granular Materials Through a Plane Hopper," *Geotchnique,* Vol. 28, No. 1, 1978, p. 27.

7 O'Callaghan, J. R., "Internal Flow in Moving Beds of Granular Materials," *Journal Agr. Engng. Res.,* Vol. 5, 1960, p. 200.

8 Gardner, G. C., "The Region of Flow When Discharging Granular Materials From Bins," *Chemical Engineering Science,* Vol. 21, 1966, p. 261.

9 Brown, R. L., and Richards, J. C., *Principles of Powder Mechanics,* Pergamon Press, 1970.

10 Wieghardt, K., "Experiments in Granular Flow," *Annual Review of Fluid Mechanics,* Vol. 7, 1975, p. 89.

11 Toyama, S., "The Flow of Granular Materials in Moving Beds," *Powder Technology,* Vol. 4, 1970–1971, p. 214.

12 Levinson, M., Shmutter, B., and Resnick, W., "Displacement and Velocity Field in Hoppers," *Powder Technology,* Vol. 16, 1977, p. 29.

13 Walker, D. M., "A Basis for Bunker Design," *Powder Technology,* Vol. 1, 1967, p. 228.

14 Eckhoff, R. K., and Leversen, P. G., "A Further Contribution to the Evaluation of the Jenike Method for Design of Mass Flow Hoppers," *Powder Technology,* Vol. 10, 1974, p. 51.

15 Wright, H., "An Evaluation of the Jenike Bunker Design Method," ASME *Journal of Engineering for Industry,* Vol. 95, 1973, p. 48.

16 Van Zanten, D. C., Richards, P. C., and Mooiji, A., "Bunker Design—Part 3: Wall Pressures and Flow Patterns in Funnel Flow," ASME *Journal of Engineering for Industry,* Vol. 99, 1977, p. 819.

17 McCabe, R. P., "Flow Pattern in Granular Material in Circular Silos," *Geotechnique,* Vol. 24, 1974, p. 45.

18 Giunta, J. S., "The Study of Flow Patterns of Granular Solids in Flat-Bottom Bins With Circular Openings," MS Thesis, University of Pittsburgh, 1966.

19 Novosad, J., and Surapati, K., "Flow of Granular Materials: Determination and Interpretation of Flow Patterns," *Powder Technology,* Vol. 2, 1968–1969, p. 82.

20 Pearce, J. C., "Mechanics of Flowing Granular Media," PhD Thesis, California Institute of Technology, 1976.

21 Crewdson, B. J., Ormond, A. L., and Nedderman, R. O., "Air Impeded Discharge of Fine Particles From a Hopper," *Powder Technology,* Vol. 16, 1977, p. 197.

22 Johanson, J. R., and Colijin, H., "New Design Criteria for Hoppers and Bins," *Iron and Steel Engineer,* Oct. 1964, p. 85.

23 Bosley, J., Schofield, C. and Shook, C. A., "An Experimental Study of Granular Discharge From Model Hoppers," *Transactions of the Institution of Chemical Engineers,* Vol. 47, 1969, p. T147.

24 Nguyen, T. V., "Studies in the Flow of Granular Materials," PhD Thesis, California Institute of Technology, Pasadena, Calif., 1979.

25 Nguyen, T. V., Brennen, C., and Sabersky, R. H. "Funnel Flow in Hoppers," *Mechanics Applied for the Transport of Bulk Materials,* ASME, AMD, Vol. 31, 1979, p. 25.

26 Savage, S. B., and Sayed, M., "Gravity Flow of Cohensionless Granular Materials in Wedge-Shaped Hoppers," *Mechanics Applied to the Transport of Bulk Materials,* ASME, AMD, Vol. 31, 1979, p. 1.